



Preparation of Poly (N-Isopropylacrylamide) -Poly (2-Ethyl-2-Oxazoline) and Their Self-Assembly Properties with Dicarboxylic Acid

Perihan Yilmaz Erdogan¹ , Fatma Bilge Emre^{2*} , Turgay Seçkin³ 

¹Gaziantep University, Department of Chemistry, Sehitkamil, 27310 Gaziantep, Türkiye

²İnönü University, Faculty of Education, Department of Mathematics and Science Education, 44280, Battalgazi/Malatya, Türkiye

³İnönü University, Faculty of Science and Literature, Department of Chemistry, 44280, Battalgazi/Malatya, Türkiye

Abstract: This study reports the synthesis of copolymers that contain thermally responsive polymers, namely poly(N-isopropylacrylamide) (PNIPAM) and poly(2-ethyl-2-oxazoline) (PEOX), as well as biodegradable side groups that are water-soluble and capable of hydrogen bonding. The assay aims to produce heat-responsive PNIPAM and PEOX polymers with di-carboxylic acid (DCA) controlled structuring of the resulting pH-sensitive nano-structured polymers. These will be used as a template in the synthesis of inorganic materials. The study demonstrated the impact of pH, salt concentration, and temperature on the polymer/DCA. This fragment describes the functional groups of the thermosensitive polymers PNIPAM and PEOX. These polymers have carboxylic acid functional groups at both ends, are water soluble, and are capable of hydrogen bonding. The structure of these polymers can be recognized with small molecules of DCA in an aqueous solution at different pH, salt concentrations, and temperatures with H-bonds. Additionally, these polymers can be used as templates to synthesize hollow silica polymers. The synthesized monomers and polymers were structurally characterized using Fourier transform infrared spectrophotometer (FT-IR). The resulting structured polymers were identified by scanning electron microscopy and atomic force microscopy (SEM, AFM). UV-VIS spectrophotometer and Differential Scanning Calorimetry (DSC) were used to determine the Lower Critical Solution temperature of the polymers.

Keywords: Self-organization, pH-sensitivity, nano-structured material, template.

Submitted: November 25, 2022. **Accepted:** February 5, 2024.

Cite this: Yilmaz Erdogan P, Emre FB, Seçkin T. Preparation of Poly (N-Isopropylacrylamide) -Poly (2-Ethyl-2-Oxazoline) and Their Self-Assembly Properties with Dicarboxylic Acid. JOTCSA. 2024;11(2):813-24.

DOI: <https://doi.org/10.18596/jotcsa.1150117>

***Corresponding author.** E-mail: fatma.emre@inonu.edu.tr

1. INTRODUCTION

Smart polymeric materials, also known as stimuli-responsive polymers, have emerged as a dynamic and innovative class of materials that can adapt their physical and chemical properties in response to external stimuli and have vast potential for technological applications (1). The remarkable feature of these systems is that they respond dramatically (solubility, shape, volume, surface properties, etc.) to slight changes in the surrounding environment, such as temperature, pH, ionic power, electrical potential, and light (2). This distinguishing feature of materials lies in rapid and drastic changes in structures and physical properties and their reversal. For some applications, a physical stimulus such as temperature is preferred to

increase the number of degenerations. It offers high-potential applications such as thermo-reactive block copolymers, temperature sensors, thermo-responsive gels, actuators, and suspending agents for distribution systems (3,4).

The thermal sensitivity of these materials is usually based on a sharp change in solubility. On heating or cooling, that is, the lower critical solution temperature (LCST) (5) or upper critical solution temperature (UCST), two distinct phase transition phenomena observed in certain polymer solutions (6). They refer to specific temperature points at which significant changes in the solution's properties occur. These phase transitions can be finely tuned by adjusting factors such as polymer chemistry, molecular weight, and the nature of the solvent. The

LCST and UCST properties of polymer solutions have found applications in a variety of fields, including drug delivery (7), thermoresponsive materials (8), and biomaterials (9), where precise control over phase behavior is essential for specific functions and applications.

PNIPAM and PEOX are well-known polymers exhibiting LCST behavior in aqueous solutions (10). LCST behavior is characterized by a phase transition from a soluble, single-phase state to a phase-separated state as the temperature of the solution is increased. PNIPAM's LCST behavior has been extensively studied and is widely used in various applications, including drug delivery systems (7), temperature-responsive hydrogels (11), and a model system for understanding LCST behavior in polymers. PEOX is less commonly studied than PNIPAM but has potential applications in drug delivery, responsive materials, and other areas (12) where LCST behavior can be advantageous. It's worth noting that the LCST behavior of these polymers can be influenced by factors such as polymer molecular weight, concentration, and the presence of additives or salts in the solution.

Polymers with carboxyl groups (-COOH) and polymers with amide groups (-CONH-) both engage in hydrogen bonding (H-bonding) interactions, but their H-bonding behaviors differ due to variations in their chemical structures (13). Carboxyl groups possess dual functionality, serving as both H-bond donors (via the -OH group) and acceptors (via the carbonyl oxygen, C=O). This dual nature results in the formation of strong H-bonds, contributing to the high-water solubility and ionization behavior of carboxyl-containing polymers. In contrast, amide groups contain both H-bond donor (-NH) and acceptor (C=O) sites, facilitating moderately strong H-bonds. These interactions play a role in the structural stability and biological compatibility of polymers featuring amide groups, such as poly(lactic-co-glycolic acid) (PLGA), which is widely employed in drug delivery and tissue engineering applications. In summary, while carboxyl groups form robust H-bonds, amide groups form moderately strong H-bonds, each imparting unique properties and applications to the respective polymers. The layer-by-layer (LbL) film formation method separates the aqueous solution of the polymer with amide groups from the aqueous solution of the polymer with carboxyl groups and alternately solid surface. It provides relatively more regular layer-to-layer film formation on solid surfaces by allowing it to be adsorbed on them, but these films do not form spontaneous (ordered) nanostructures because the polymers adsorbed on the surfaces are kinetically trapped and their mobility is limited (14). However, water-soluble polymers can be made with weak physical interactions in dilute solutions. It is known that amide groups can form H-bond with carboxyl groups in aqueous solutions (15). In light of the information that this interaction can be successfully used in layer-by-layer pH-sensitive film formation and the

water-soluble polymers can be made with weak physical interactions in dilute solutions (16). PNIPAM and PEOX polymers were chosen as the model system. PNIPAM and PEOX are heat-reactive polymers that exhibit subcritical solution behavior. PNIPAM is highly soluble in water, and the solution appears clear and homogeneous. Above the LCST (above approximately 32°C), the polymer undergoes a phase transition, becoming increasingly insoluble in water. This results in the formation of polymer-rich aggregates or a separate polymer-rich phase, leading to cloudiness or phase separation in the solution. Similar to PNIPAM, PEOX exhibits LCST behavior in aqueous solutions. Below the LCST, PEOX is soluble in water, and the solution is clear. Above the LCST (above approximately 61°C), PEOX undergoes a phase transition, leading to reduced solubility and phase separation. Both polymers are completely dissolved in water under LCST, and polymer chain conformations can be controlled between the two expanded and contracted endpoints (17). On the LCST, the polymer chains are in the form of globules. As a result of breaking the H-bonds formed with water on the LCST, phase separation is observed, and the solution becomes cloudy. Poly(2-ethyl-2-oxazoline) self-assembles in a phase-decomposed solution on LCST and forms copolymer (18). When looking at the structuring of PEOX in aqueous solutions, it has been shown that crystalline PEOX polymers were formed on LCST. The basic mechanism in the formation of these crystalline polymers is the orientation of the amid dipoles in the PEOX chains as a result of strong dipolar interactions. PNIPAM is stable in aqueous solution above and below the LCST and is not structured (19,20).

Maleic acid, a dicarboxylic organic acid, possesses several properties that make it of interest in applications involving LCST behavior and responsive polymers. The pKa1 and pKa2 values of maleic acid are important in understanding its behavior in LCST systems, especially when it influences the pH of the solution and thereby impacts the LCST of responsive polymers. Maleic acid has two pK, which are pKa1 (the first ionization constant), which was approximately 1.9, and pKa2 (the second ionization constant), which was approximately 6.3. These pKa values indicate the pH levels at which specific ionization states of maleic acid occur. The first pKa (pKa1) corresponds to the ionization of the first carboxyl group (-COOH) in maleic acid, resulting in the formation of the maleate anion (-COO-). The second pKa (pKa2) represents the ionization of the second carboxyl group in maleic acid, leading to the formation of the dihydrogen maleate anion (-HCOO-). In LCST systems, maleic acid can be added to solutions to adjust the pH, and this adjustment can influence the LCST behavior of responsive polymers like PNIPAM and PEOX. Depending on the pH of the solution, the ionization states of maleic acid can vary, which, in turn, can affect the interactions between maleic acid and the polymers, leading to alterations in the LCST. By knowing the pKa1 and pKa2 values of maleic acid, researchers can control

and tailor the pH conditions in LCST systems, allowing for precise manipulation of the LCST behavior of responsive polymers, which is particularly useful in applications such as drug delivery systems and responsive materials. Figure 1

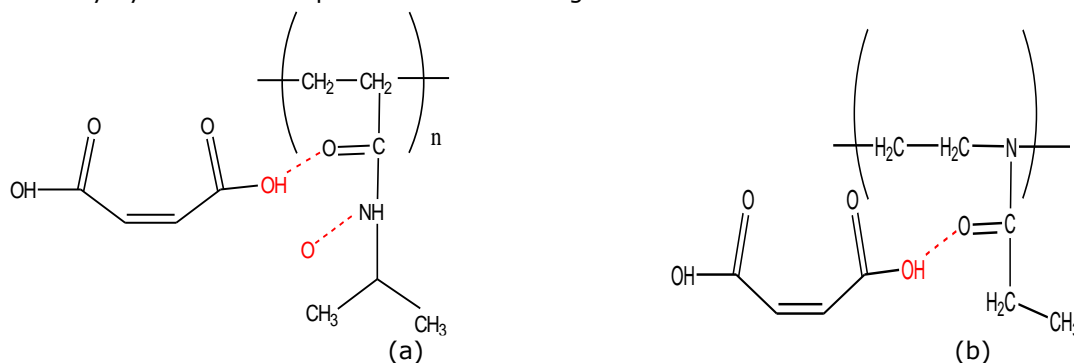


Figure 1: H-bonds of maleic acid with thermally reactive polymers in the range $pK_{a1} < pH < pK_{a2}$: a) PNIPAM, b) PEOX.

Both polymers have amide (= N-C = O) functional groups. It is well-known and widely studied that amide groups make H-bonds with carboxylic acid (-COOH) groups (21). In the amide group, both carbonyl (-C = O) and nitrogen (N) groups can be H-accepting (H-acceptor) H-bonds. Secondary amine-NH groups in PNIPAM are also H-donors. PEOX has tertiary amine -N = groups, no H-donor (-CH₃ and =CH₂ do not act as H-donors in aqueous solution). Intermolecular and intramolecular H-bonds are formed due to the co-presence of H-acceptor and H-donor groups in PNIPAM. These H-bonds are the reason for the hysteresis observed in the thermal reaction transition around the LCST in PNIPAM aqueous solutions (22). Working together on the self-assembly of PNIPAM and PEOX with DCAs and comparing the results with each other will enable us to understand the effects of different polymer chemical structures and different thermal response behaviors (having different LCST) on self-assembly in aqueous solutions.

Poly(N-isopropylacrylamide) (PNIPAM), poly(2-ethyl-2-oxazoline) (PEOX), and maleic acid are substances that have garnered significant scientific interest due to their pivotal roles in lower critical solution temperature (LCST) behavior, which triggers remarkable phase transitions in response to environmental changes. LCST represents a critical point at which these polymers switch from being soluble to forming aggregates or phase-separated structures, rendering them invaluable in applications requiring precise control over responses to factors like temperature and pH. Understanding the interplay between these compounds and their influence on LCST is paramount, as it underpins innovations in drug delivery systems, responsive materials, and a myriad of fields where controlled phase transitions are crucial for functionality and performance.

This study aimed to synthesize copolymers containing thermally responsive polymers ((poly (N-isopropylacrylamide) (PNIPAM) and poly (2-ethyl-2-

shows the H-bonds maleic acid will make with thermally reactive polymers in the range $pK_{a1} < pH < pK_{a2}$.

oxazoline) (PEOX)) and biodegradable side groups which are water soluble and capable of hydrogen bonding for using biomedical applications.

2. EXPERIMENTAL SECTION

2.1. Materials and Equipment

NIPAM ($\geq 97\%$, 113.16 g/mol), PEOX (MW: 200.000 g/mol), maleic acid ($\geq 99\%$, HPLC, 116.07 g/mol), Potassium persulfate (ACS reagent, $\geq 99.0\%$, 270.32 g/mol), Sodium iodide (ACS reagent, $\geq 99.0\%$, 149.89 g/mol), Sodium chloride (ACS reagent, $\geq 99.0\%$, 58.44 g/mol), Sodium sulfate (ACS reagent, $\geq 99.0\%$, anhydrous, granular, 142.04 g/mol) and Sodium carbonate (ACS reagent powder, $\geq 99.5\%$, 105.99 g/mol) were purchased from Sigma Aldrich. All chemicals were used without purification.

Perkin Elmer model Fourier Transform Infrared Spectrophotometer (FT-IR), Leo EV40 SEM, Park Systems XE-100E label AFM, Shimadzu UV-1601 model UV-VIS spectrophotometer, and Shimadzu DSC-60 model Differential Scanning Calorimetry were used.

2.2. Synthesis of Poly (N-isopropylacrylamide) (PNIPAM)

To synthesize 0.02 mol PNIPAM, 2.5 g of NIPAM was placed in a tube, and 31.25 mL of distilled water was added to it. NIPAM was mixed with a magnetic stirrer at room temperature until completely dissolved. Then, 0.125 g of Potassium persulfate initiator was added, the tube was placed in the oil bath, and it was kept in the oil bath and magnetic stirrer for 2 hours at a constant temperature (70 °C) for the polymerization to occur. In this way, PNIPAM polymer is obtained.

2.3. Characterization

Perkin Elmer model FT-IR was used for the structural characterization of the synthesized monomers and polymers. During these analyses, FT-IR measurements were made in the 400-4000

cm⁻¹ wave number range and with an ATR surface scanning system. Leo EV40 SEM device was used for surface properties to magnify the image. Park Systems XE-100E brand AFM was used to determine the surface topography of the polymers obtained. Shimadzu UV-1601 brand UV-vis spectrophotometer and Shimadzu DSC-60 brand Differential Scanning Calorimeter were used to determine the subcritical solution temperature of the polymers.

3. RESULTS AND DISCUSSION

3.1. Self-assembly of PNIPAM and PEOX Polymers with Dicarboxylic Acid Solution

Figure 2 illustrates the different amounts of 0.02 mol PNIPAM (a: 2 mg, b: 4 mg, c: 6 mg, d: 8 mg, e: 10 mg) in 0.8M maleic acid solution at different pH (2, 4, 6, 8, 10) configuration. The structuring of PNIPAM and PEOX polymers in aqueous solution was

carried out through H-bonds with maleic acid. To do this, we either use the polymer chain in the range $pK_{a1} < pH < pK_{a2}$ as described above, and the chain of electrostatic interactions is stretched, or we need to find the pH where the pH is less than pK_{a1} and the corresponding pH where a carboxylic acid is protonated. Maleic acid solutions were prepared at different pH (2, 4, 6, 8, 10) values and were used for this. A constant amount of this solution was put into the tube. PNIPAM maleic acid structuring was examined by adding different amounts of 0,02 mol PNIPAM (2-10 mg). Figure 2 shows no structuring at pH 2 and pH 4, while self-assembly takes place at pH 6, pH 8, and pH 10. As the polymer amount increases, the structuring between the polymer and DCA increases even more. As seen in Figure 2, the most suitable maleic acid pH for the structuring of PNIPAM has been determined as pH 6.

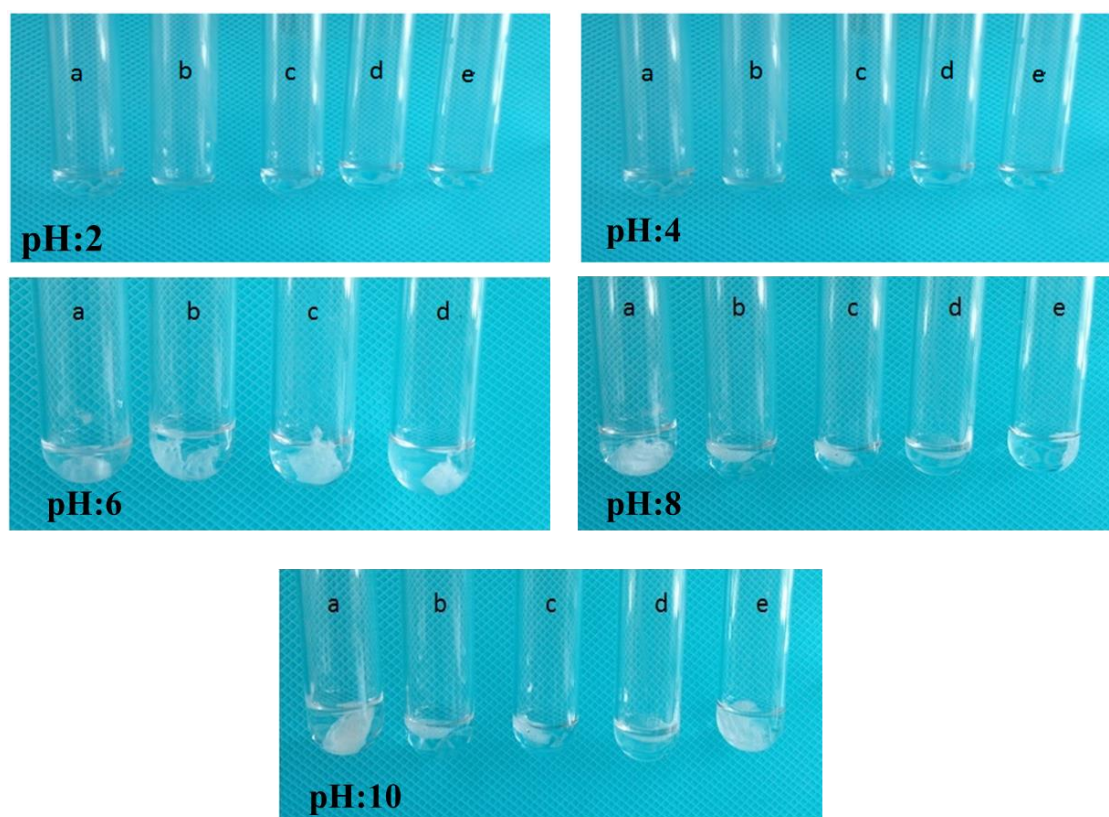


Figure 2: Structuring of a specific amount of PNIPAM polymers (a: 2 mg, b: 4 mg, c: 6 mg, d: 8 mg, e: 10 mg) in maleic acid solution with varying pH values (2, 4, 6, 8, 10).

PEOX polymer was analyzed by combining solutions of maleic acid at varying pH values. It was demonstrated in Figure 3 shows the configuration of the PEOX polymer in the maleic acid solution at

three different pH values (a: 6, b: 8, c: 10). As a result of the experiments, we see that the structuring of PEOX in maleic acid started at pH 8.

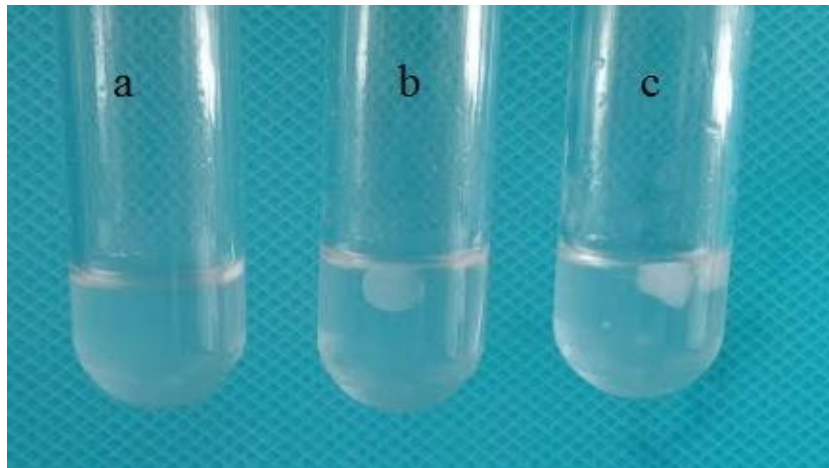


Figure 3: Structuring of the PEOX polymer in maleic acid solution at different pH (a: 6, b: 8, c: 10).

3.2. Self-assembly of Maleic Acid and PEOX and PNIPAM Mix

The structuring of PEOX and PNIPAM polymers in maleic acid was examined separately. Copolymerization of NIPAM with special pH value-responsive and strong hydrophilic ability of PEOX results in dual pH and temperature-stimuli-

responsive hydrogels. The determined LCST values of the copolymer obtained from different ratios of PEOX and PNIPAM in maleic acid solution are given in Table 1. Table 1 can be used to determine the optimal gel ratio and temperature for *in vivo* research or biomedical applications.

Table 1: Gel ratio of PEOX - PNIPAM blend.

Blend	% (V/V)	LCST (°C)
1.PEOX-PNIPAM	90-10	32
2.PEOX-PNIPAM	80-20	32
3.PEOX-PNIPAM	70-30	34
4.PEOX-PNIPAM	60-40	35
5.PEOX-PNIPAM	50-50	35
6.PEOX-PNIPAM	40-60	36
7.PEOX-PNIPAM	30-70	36
8.PEOX-PNIPAM	20-80	37
9.PEOX-PNIPAM	10-90	40

Figure 4 shows the structuring of the blend of PEOX and PNIPAM in maleic acid solution at different pH (a) pH:5, b) pH:5.3, c) pH:5.6, d) pH:5.8, e) pH:6,

f) pH:8, g) pH:10). The structuring of PEOX and PNIPAM blend in maleic acid solution at different pH starts at approximately pH 5.8.

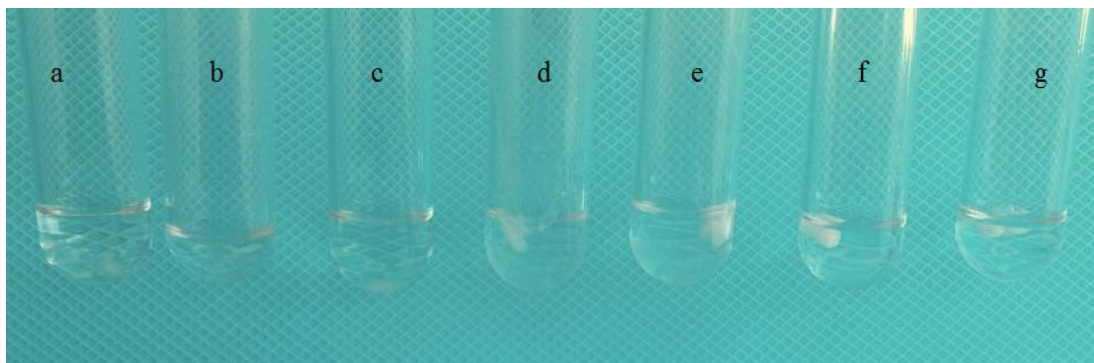


Figure 4: Maleic acid structuring of PEOX and PNIPAM blend at different pH; a) pH:5, b) pH:5.3, c) pH:5.6, d) pH:5.8, e) pH:6, f) pH:8, g) pH:10).

3.3. Determination of Sub-Critical Solution Temperature of PNIPAM and PEOX Polymers

"Smart" materials, in other words, materials that can react to stimuli, represent one of the darkest classes of materials (23). There are two basic types of thermo-reactive polymers; The first presents the LCST, while the second presents the UCST (24). For example, a polymer solution below MAP is a clear, homogeneous solution; A polymer solution above

LCST looks cloudy (also known as LCST's cloud point). Figure 5 a show a 32 ° C LCST of PNIPAM. This temperature is close to body temperature. This proximity is a very useful temperature for biomedical applications. Figure 5 b shows a 61 ° C LCST of PEOX. Figure 5 c shows the LCST behavior of the PEOX-PNIPAM blend against temperature. LCST temperature of 20-80% PEOX-PNIPAM blend was determined as 37 ° C.

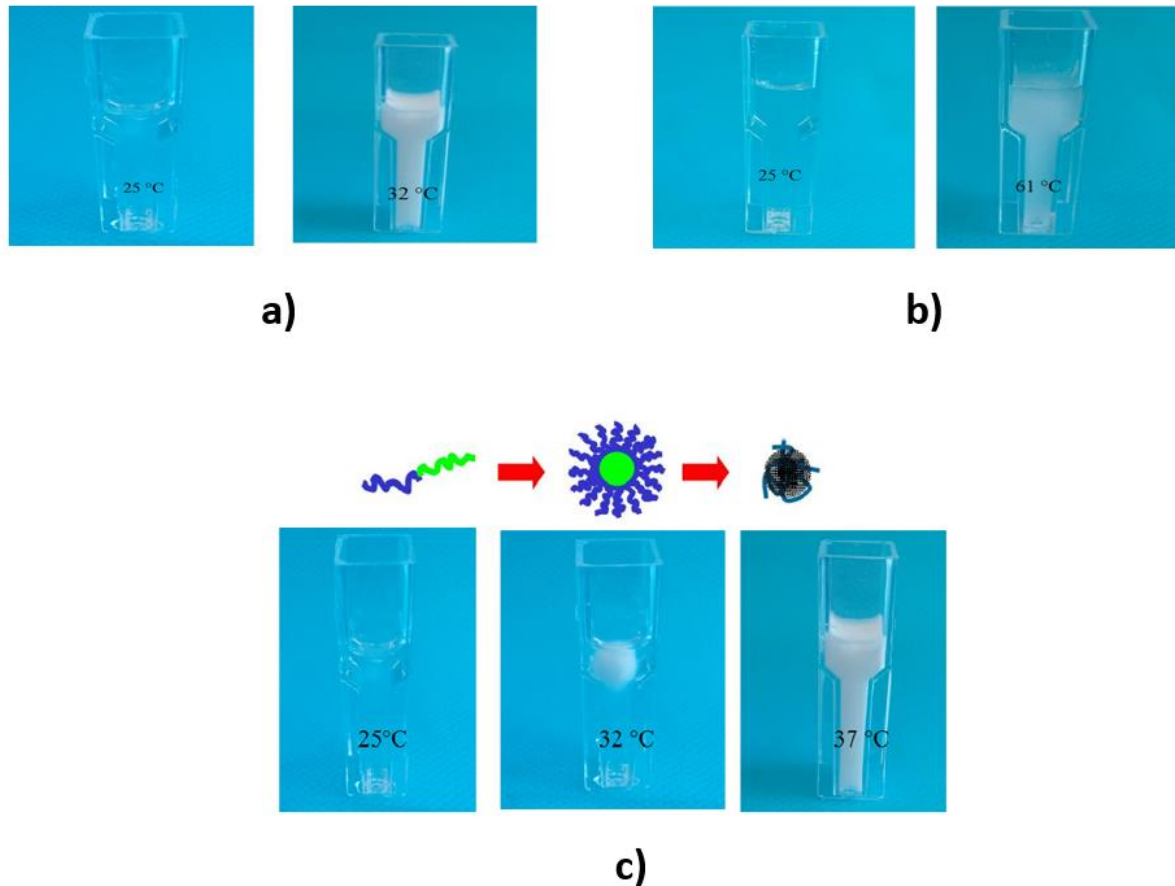


Figure 5: LCST behavior with temperature a) PNIPAM's, b) PEOX, and c) PEOX-PNIPAM blend.

3.4. Characterization

Figure 6a show the FT-IR spectrum of PNIPAM. 3292 cm^{-1} (secondary amide NH stretch) (25), 2970 cm^{-1} ($-\text{CH}_3$ asymmetric stretch) (26), 1650 cm^{-1} (secondary amide C = O stretch, amide bond) (27) and 1550 cm^{-1} O stretch, amide II bond). Figure 6b shows the FT-IR spectrum for PNIPAM-DCA configuration. Considering the polymeric structures made with DCA, the peak changes occurring - C = O peaks are seen in 1660-1735 cm^{-1} . N-H peak is seen

in 3292 cm^{-1} (28) and the aliphatic C-H strain peak is seen in 2850-2950 cm^{-1} . Possible peaks for these polymers, which are made with a hydrogen bond, are seen where expected. In these structures where structural change is observed, the structures formed due to hydrogen bonding are seen around 2300 cm^{-1} . The peaks of different shapes of hydrogen bonds indicate that the embodiment is in different shapes and some regions within the polymeric chain.

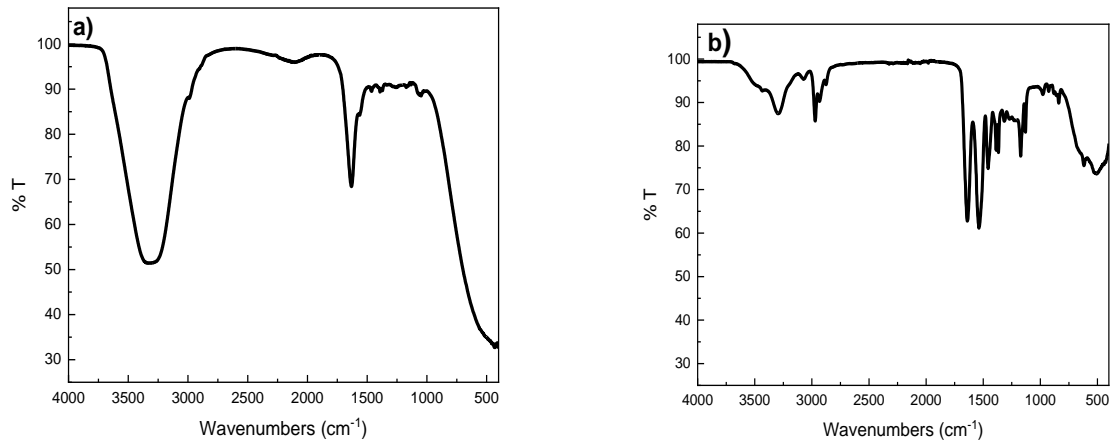


Figure 6: FT-IR spectrum of a) PNIPAM and b) Self-assembly of PNIPAM-DCA.

Figure 7 shows the UV-VIS graphic for PNIPAM. As a result of the studies, the LCST UV-VIS spectrophotometer measurement technique is determined for PNIPAM. For PNIPAM, LCST is available at 32 °C. Figure 7 b shows the DSC results

for PNIPAM. For PNIPAM, LCST is measured this time with the DSC technique. For PNIPAM, LCST also supports literature and the UV-VIS spectrophotometer measurement technique, which is determined to be 32 °C (29).

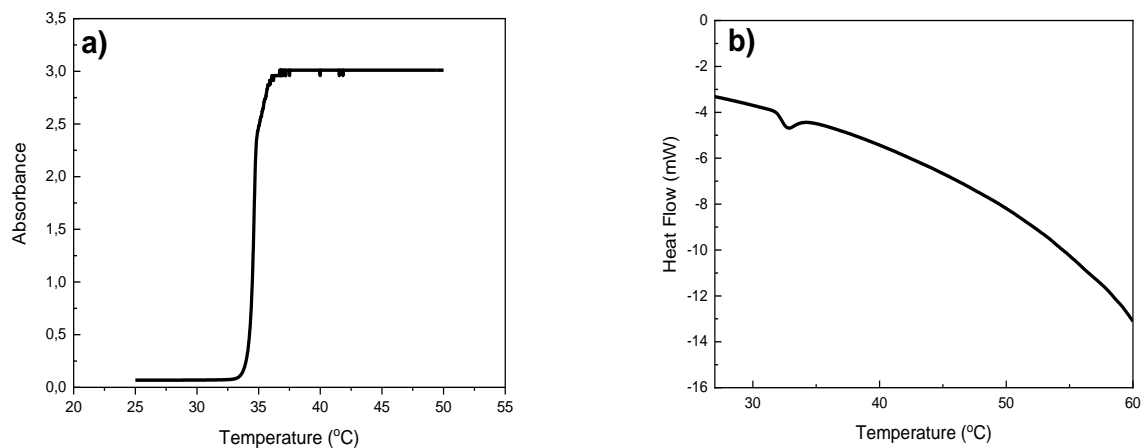


Figure 7: a) UV-VIS and b) DSC thermogram of PNIPAM structure

Figure 8 shows AFM images at different magnifications for PNIPAM-DCA configuration. When AFM images of the gel structures obtained in the studies are examined, it is thought that possible configurations are caused by interactions such as van der Waals forces, electrostatic interactions, entropic forces, steric forces, and external volume

repulsion (30). The stability of the colloidal system is used in the sense of suspending the particles in the solution, that is, suspending. Stability decreases with aggregation and precipitation phenomenon. These facts are disclosed due to the tendency to reduce surface energy. Reduced surface tension ensures colloidal particles are stable.

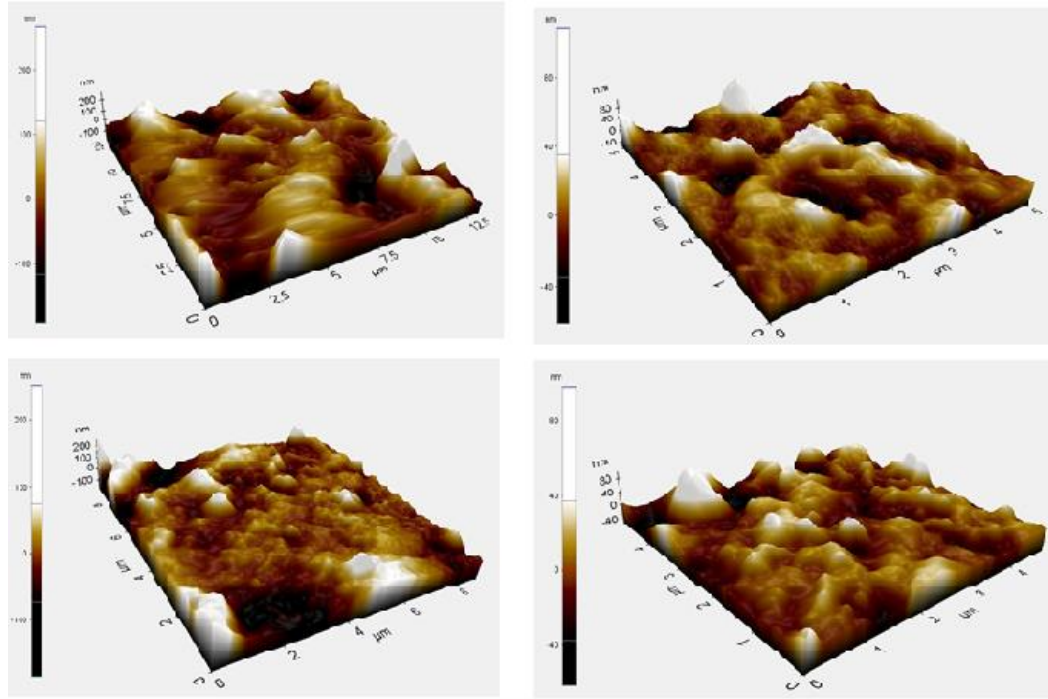


Figure 8: AFM images for PNIPAM-DCA configuration.

Clumping is actually the sum of the forces of attraction between the particles. If the gravitational forces, for example, van der Waals, are greater than the thrust forces, the particles come together to clump together. Electrostatic and steric settling prevents the agglomeration and collapse of the

particle. Therefore, it is understood that possible interactions arise from these forces. AFM images are capable of supporting this. The initial structure and possible pore diameters change after the interaction process, and the formation of nanostructures are given in AFM images (31).

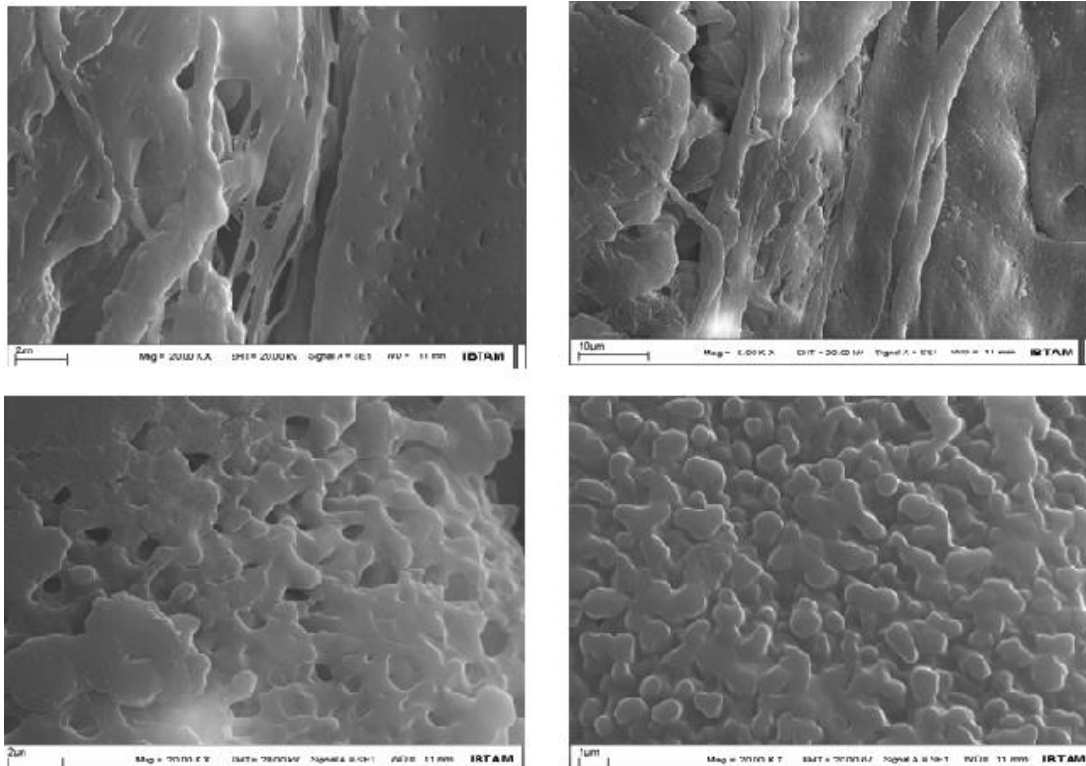


Figure 9: SEM images of self-assembly of PNIPAM-DCA (20.00 KX magnification).

Figure 9 shows SEM images in different magnifications for PNIPAM-DCA structuring. When

SEM images are examined, it is seen that PNIPAM structures with DCA functionality are constructed in

the form of bars and there are gaps in the intermediate segments. When the results of SEM structural analysis are interpreted as equivalent to AFM images, the effect of the constructions on the morphology is understood. Among the polymeric embodiments, the regional hydrogen bond shows that the structure interacts with the overlap and ball. Globule formations can be converted back to the old heap by changing the environment

variables. The most important evidence of this transformation is that the structural dissolution event and the clarification and collapse, i.e. self-structuring, are reversible. It is clearly seen that when the high magnifications of the building are reached, their surfaces have a clear gap. All these properties prove that the synthesized structures have porous morphology.

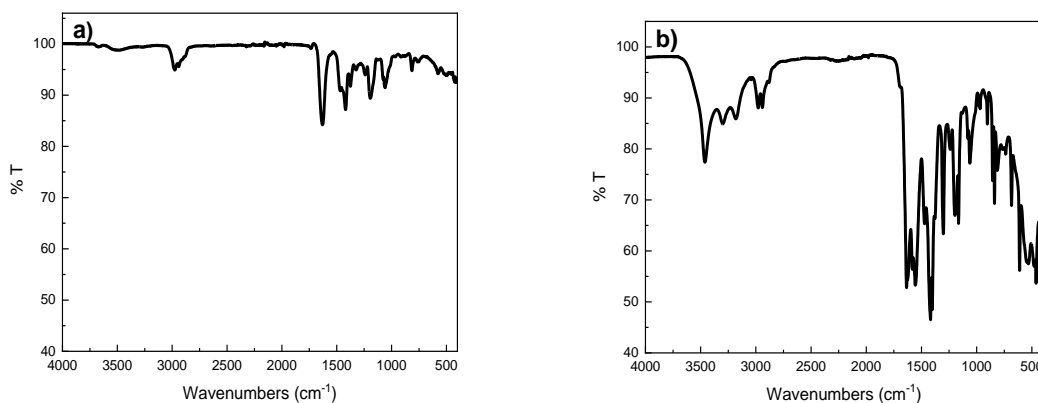


Figure 10: FT-IR spectrum of a) PEOX b) Self-configuration of PEOX-DCA.

Figure 10a shows the FT-IR spectrum of the PEOX structure. At 2820-3100 cm^{-1} we see the peak caused by the aliphatic C-H groups in the structure, at 1620 cm^{-1} we see the carbonyl stress peak vibration. In addition, the C-C tensile peak at 1370 cm^{-1} and aliphatic CH_2 vibration peak from CH_2 groups are seen at 1180 cm^{-1} (32). All these structures are compatible with the literature, and the desired PEOX structure has been reached.

Figure 10 b shows the FT-IR spectrum for the PEOX-DCA configuration. In this structure, we also see carbonyl stress vibrations caused by DCA attached to the structure. The secondary carbonyl peak at 1520 cm^{-1} was included in the spectrum (33). In addition, the characteristic structure of the C-H tension peak in the structure has changed, and this change proves that DCA is connected to the structure.

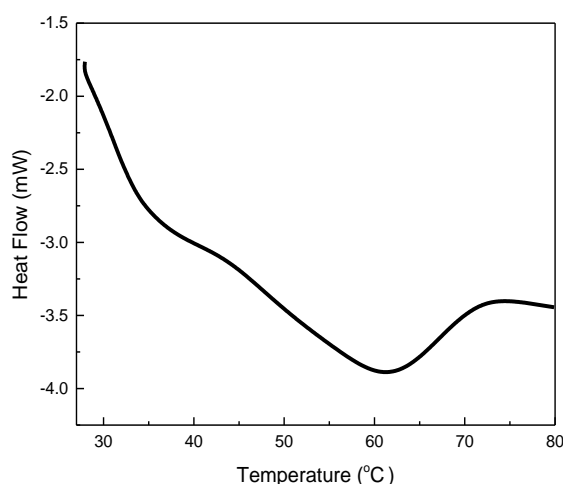


Figure 11: DSC thermogram for PEOX.

Figure 11 shows the DSC thermogram for PEOX. The LCST of the PEOX structure was determined as 61.78 $^{\circ}\text{C}$. The behavior of the building against temperature is reversible. Figure 12 shows the different magnification AFM images of the polymers

obtained by connecting DCA to the PEOX structure. Homogeneous and smooth porosity was determined in the structure at different magnifications. The gaps in Figure 12 show us that DCA and PEOX form a very regular structure.

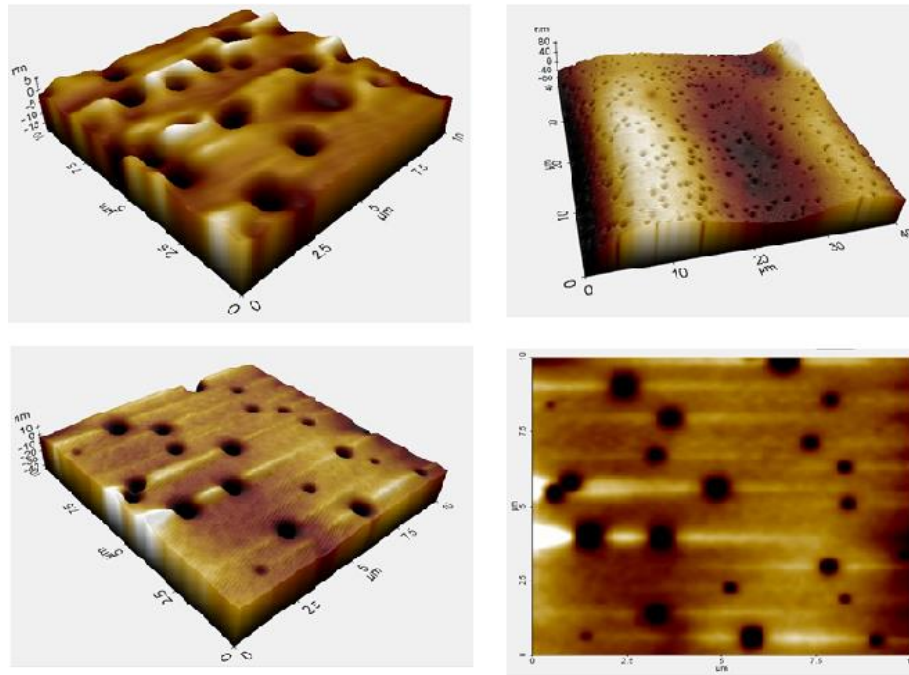


Figure 12: AFM images for PEOX-DCA structuring.

The FT-IR spectrum of the PEOX-PNIPAM blend is presented in Figure 13a. The FT-IR spectrum of the DCA configuration of the PEOX-PNIPAM blend is presented in Figure 13b. The spectrum shows that the most significant change is the carbonyl peak at 1520 cm^{-1} , originating from the DCA structure.

Additionally, there are carbonyl tensile vibrations at 1620 cm^{-1} from PNIPAM and at $1630\text{--}1620\text{ cm}^{-1}$ from the PEOX structure (34). It is important to note that all three carbonyl peaks are desired to coexist in the structure.

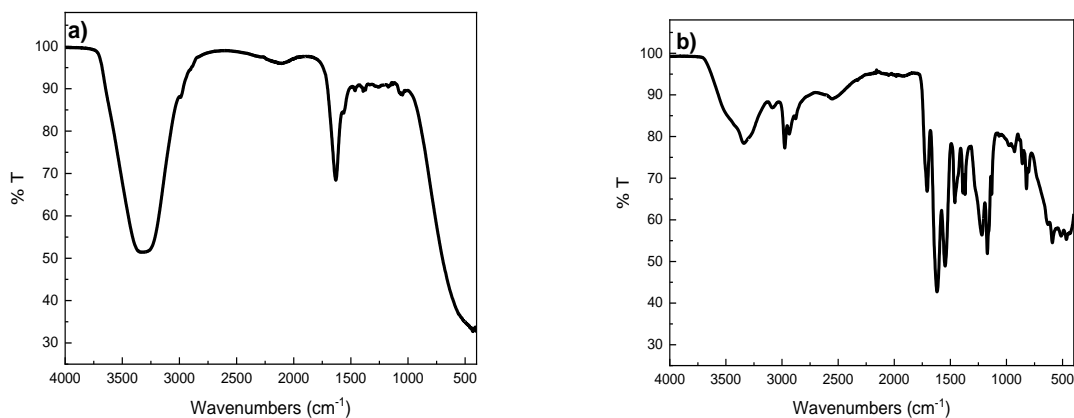


Figure 13: FT-IR spectrum of a) PEOX-PNIPAM blend, b) PEOX-PNIPAM-DCA structuring.

Figure 14 displays the AFM images for the DCA configuration of the PEOX - PNIPAM blend. The clusters on the surface and the rough surface image

indicate that DCA is connected to the PEOX-PNIPAM structure, as shown in the AFM images.

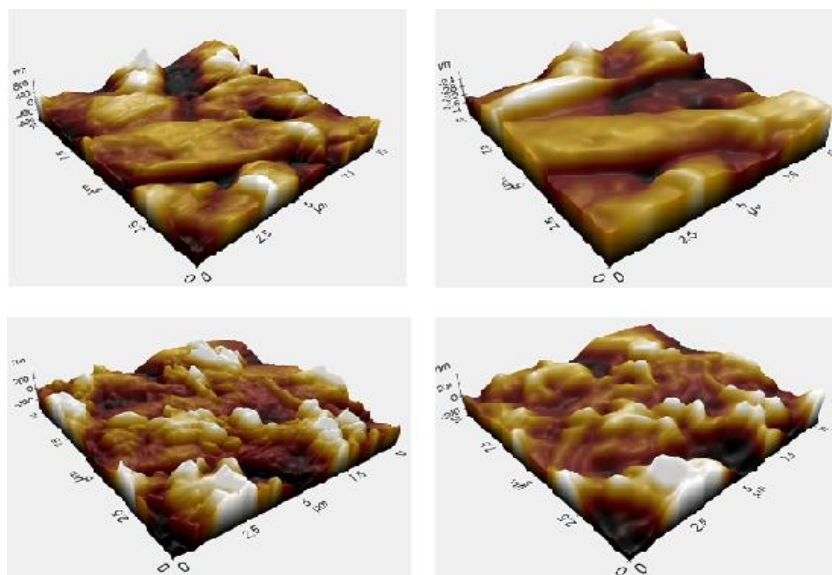


Figure 14: AFM images of PEOX – PNIPAM blend DCA structuring.

4. CONCLUSION

After synthesizing PNIPAM and conducting structural characterization, the LCST value was determined using DSC and UV-VIS. The structuring of PNIPAM with maleic acid (DCA) was then examined. PNIPAM and PEOX polymers were blended in specific proportions, and their LCST behaviors were systematically analyzed. It was discovered that changes greatly influenced the LCST behavior of the blend in hydrophobicity. The addition of PEOX to PNIPAM increased the LCST value. The repeating units of PNIPAM have both hydrophobic and hydrophilic parts. At low temperatures, strong hydrogen bonds form between hydrophilic groups in the polymer and water molecules, which counteract the unwanted free energy caused by the interaction of hydrophobic groups with water molecules. This allows the polymer to dissolve well in water. As the temperature increases, hydrophobic interactions between hydrophobic side groups become stronger while hydrogen bonding weakens. At temperatures above the LCST, interactions between hydrophobic groups dominate. Entropy-induced failure and phase separation are observed in polymer chains. The decrease in the movement of the polymer chains is compensated for by the increase in entropy resulting from the separation of the polymer from a high order around its hydrophobic groups. Therefore, increasing or decreasing the hydrophilic content of PNIPAM results in an increase or decrease in the LCST value, respectively. It is important to understand that the LCST is dependent on both the salt concentration and the molecular mechanisms that cause this behavior. This understanding is crucial for adjusting the LCST as desired for various applications. The present study examined the structures of PNIPAM, PEOX, and PEOX-PNIPAM blends with maleic acid and determined their pH sensitivity.

5. CONFLICT OF INTEREST

The authors state no conflict of interest.

6. ACKNOWLEDGMENTS

This work was supported by Inonu University, BAP 2016-13

7. REFERENCES

- Pino-Ramos VH, Ramos-Ballesteros A, López-Saucedo F, López-Barriguete JE, Varca GHC, Bucio E. Radiation grafting for the functionalization and development of smart polymeric materials. In: Applications of Radiation Chemistry in the Fields of Industry, Biotechnology and Environment. Springer; 2017. p. 67–94.
- Wei M, Gao Y, Li X, Serpe MJ. Stimuli-responsive polymers and their applications. *Polym Chem.* 2017;8(1):127–43. Available from: [URL](#)
- Karimi M, Sahandi Zangabad P, Ghasemi A, Amiri M, Bahrami M, Malekzad H, et al. Temperature-responsive smart nanocarriers for delivery of therapeutic agents: applications and recent advances. *ACS Appl Mater Interfaces.* 2016;8(33):21107–33. Available from: [URL](#)
- Li J, Kikuchi S, Sato S ichiro, Chen Y, Xu L, Song B, et al. Core-First Synthesis and Thermoresponsive Property of Three-, Four-, and Six-Arm Star-Shaped Poly (N, N-diethylacrylamide)s and Their Block Copolymers with Poly (N, N-dimethylacrylamide). *Macromolecules.* 2019;52(19):7207–17. Available from: [URL](#)
- Al-Zaidi AT, Al-Dokheily ME, Al-Atabi SH. Low critical solution temperatures and water swelling ratios of some new PNIPAAm copolymers synthesized by free radical polymerization. In: AIP Conference Proceedings. AIP Publishing LLC; 2020. p. 20176.
- Tseng W, Fang T, Chen C, Hsieh Y, Lai W. Upper Critical Solution Temperature-Type Thermal Response of Soluble Multi-l-Arginyl-Poly-l-Aspartic Acid (cyanophycin) Conjugated with Maltodextrin. *J Polym Sci A Polym Chem.* 2019;57(19):2048–55. Available from: [URL](#)

7. Pasparakis G, Tsitsilianis C. LCST polymers: Thermoresponsive nanostructured assemblies towards bioapplications. *Polymer*, 2020; 211: 123146. Available from: [URL](#)
8. Marsili L, Dal Bo M, Berti F, Toffoli G. Chitosan-Based Biocompatible Copolymers for Thermoresponsive Drug Delivery Systems: On the Development of a Standardization System. *Pharmaceutics*. 2021; 13(11): 1876. Available from: [URL](#)
9. Kocak G, Tuncer C, Bütün V. Stimuli-Responsive Polymers Providing New Opportunities for Various Applications. *Hacetatepe J. Biol. & Chem.*, 2020; 48(5): 527-574. Available from: [URL](#)
10. Konefał R, Spěváček J, Černoch P. Thermoresponsive poly (2-oxazoline) homopolymers and copolymers in aqueous solutions studied by NMR spectroscopy and dynamic light scattering. *Eur Polym J*. 2018; 100: 241-52. Available from: [URL](#)
11. Tang Q, Qian S, Chen W, Song X, Huang J. Preparation and characterization of temperature-responsive Ca-alginate/poly(N-isopropylacrylamide) hydrogel. *Polym Int*, 2023; 72: 252-262. Available from: [URL](#)
12. Lusina A, Nazim T, Cegłowski M. Poly(2-oxazoline)s as Stimuli-Responsive Materials for Biomedical Applications: Recent Developments of Polish Scientists. *Polymers*. 2022; 14(19):4176. Available from: [URL](#)
13. Mizusaki M, Endo T, Nakahata R, Morishima Y, Yusa S ichi. pH-induced association and dissociation of intermolecular complexes formed by hydrogen bonding between diblock copolymers. *Polymers (Basel)*. 2017;9(8):367. Available from: [URL](#)
14. Zhu YG, Wang Y, Shi Y, Wong JI, Yang HY. CoO nanoflowers woven by CNT network for high energy density flexible micro-supercapacitor. *Nano Energy*. 2014;3:46-54. Available from: [URL](#)
15. Altıntaş Z, Adatoz EB, Ijaz A, Miko A, Demirel AL. Self-assembled poly (2-ethyl-2-oxazoline)/malonic acid hollow fibers in aqueous solutions. *Eur Polym J*. 2019;120:109222. Available from: [URL](#)
16. Kocak G, Tuncer C, Bütün V. pH-Responsive polymers. *Polym Chem*. 2017;8(1):144-76. Available from: [URL](#)
17. Hendessi S, Güner PT, Miko A, Demirel AL. Hydrogen bonded multilayers of poly (2-ethyl-2-oxazoline) stabilized silver nanoparticles and tannic acid. *Eur Polym J*. 2017;88:666-78. Available from: [URL](#)
18. Oleszko-Torbus N, Utrata-Wesołek A, Bochenek M, Lipowska-Kur D, Dworak A, Wałach W. Thermal and crystalline properties of poly (2-oxazoline)s. *Polym Chem*. 2020;11(1):15-33. Available from: [URL](#)
19. Ohnsorg ML, Ting JM, Jones SD, Jung S, Bates FS, Reineke TM. Tuning PNIPAm self-assembly and thermoresponse: roles of hydrophobic end-groups and hydrophilic comonomer. *Polym Chem*. 2019;10(25):3469-79. Available from: [URL](#)
20. Gandhi A, Paul A, Sen SO, Sen KK. Studies on thermoresponsive polymers: Phase behaviour, drug delivery and biomedical applications. *Asian J Pharm Sci*. 2015;10(2):99-107. Available from: [URL](#)
21. Adams N, Schubert US. Poly (2-oxazolines) in biological and biomedical application contexts. *Adv Drug Deliv Rev*. 2007;59(15):1504-20. Available from: [URL](#)
22. Gaertner FC, Luxenhofer R, Blechert B, Jordan R, Essler M. Synthesis, biodistribution and excretion of radiolabeled poly (2-alkyl-2-oxazoline) s. *Journal of Controlled Release*. 2007;119(3):291-300. Available from: [URL](#)
23. Dutta K, De S. Smart responsive materials for water purification: an overview. *J Mater Chem A Mater*. 2017;5(42):22095-112. Available from: [URL](#)
24. Zou H, Wu Q, Li Q, Wang C, Zhou L, Hou XH, et al. Thermo-and redox-responsive dumbbell-shaped copolymers: from structure design to the LCST-UCST transition. *Polym Chem*. 2020;11(4):830-42. Available from: [URL](#)
25. Chen JJ, Ahmad AL, Ooi BS. Poly (N-isopropylacrylamide-co-acrylic acid) hydrogels for copper ion adsorption: Equilibrium isotherms, kinetic and thermodynamic studies. *J Environ Chem Eng*. 2013;1(3):339-48. Available from: [URL](#)
26. Wang J, Sutti A, Lin T, Wang X. Thermo-responsive PNIPAM hydrogel nanofibres photocrosslinked by azido-POSS. In: *Fiber Society Spring 2013 Technical Conference*. Fiber Society; 2013. Available from: [URL](#)
27. Li G, Song S, Zhang T, Qi M, Liu J. pH-sensitive polyelectrolyte complex micelles assembled from CS-g-PNIPAM and ALG-gP (NIPAM-co-NVP) for drug delivery. *Int J Biol Macromol*. 2013;62:203-10. Available from: [URL](#)
28. Lai H, Wang Z, Wu P. Structural evolution in a biphasic system: poly (N-isopropylacrylamide) transfer from water to hydrophobic ionic liquid. *RSC Adv*. 2012;2(31):11850-7. Available from: [URL](#)
29. Saad A, Mills R, Wan H, Mottaleb MA, Ormsbee L, Bhattacharyya D. Thermo-responsive adsorption-desorption of perfluoroorganics from water using PNIPAM hydrogels and pore functionalized membranes. *J Memb Sci*. 2020;599:117821. Available from: [URL](#)
30. Rusen L, Dinca V, Mustaciosu C, Icriverzi M, Sima LE, Bonciu A, et al. Smart Thermoresponsive Surfaces Based on pNIPAm Coatings and Laser Method for Biological Applications. *Modern Technologies for Creating the Thin-film Systems and Coatings*. 2017;10. Available from: [URL](#)
31. Mourdikoudis S, Pallares RM, Thanh NTK. Characterization techniques for nanoparticles: comparison and complementarity upon studying nanoparticle properties. *Nanoscale*. 2018;10(27):12871-934. Available from: [URL](#)
32. Niranjnmurthi L, Park C, Lim KT. Synthesis and characterization of graphene oxide/poly (2-ethyl-2-oxazoline) composites. *Molecular Crystals and Liquid Crystals*. 2012;564(1):206-12. Available from: [URL](#)
33. Minkova LI, Miteva T, Sek D, Kaczmarczyk B, Magagnini PL, Paci M, et al. Reactive blending of a functionalized polyethylene with a semiflexible liquid crystalline copolyester. *J Appl Polym Sci*. 1996;62(10):1613-25. Available from: [URL](#)
34. Kuo SW. Hydrogen bonding in polymeric materials. *John Wiley & Sons*; 2018. Available from: [URL](#)